Fortschr. Phys. **48** (2000) 5–7, 671–678

State Preparation by Photon Filtering

G. M. D'Ariano, L. Maccone, M. G. A. Paris, and M. F. Sacchi

Theoretical Quantum Optics Group – INFM Unitá di Pavia
Dipartimento di Fisica 'Alessandro Volta' – Universitá di Pavia
via A. Bassi 6, I-27100 Pavia, Italy

Abstract

We propose a setup capable of generating Fock states of a single mode radiation field. The scheme is based on coupling the signal field to a ring cavity through cross-Kerr phase modulation, and on conditional ON-OFF photodetection at the output cavity mode. The same setup allows to prepare selected superpositions of Fock states and entangled two-mode states. Remarkably, the detector's quantum efficiency does not affect the reliability of the state synthesis.

1. Introduction

The generation of optical radiation number (Fock) states is of importance for a number of different applications, ranging from high resolution spectroscopy to fundamental tests of Quantum Mechanics. In quantum communication, Fock states achieve the optimal capacity of quantum channels [1], whereas in optical quantum computation superpositions of Fock states are needed as input states [2]. The synthesis of Fock states also allows to experimentally characterize active optical devices [3]. In this paper, we suggest a novel preparation scheme for Fock states and their superpositions. In our proposal, a traveling wave mode is coupled to a ring cavity through cross-Kerr phase modulation. The cavity mode serves as a probe, and a successful photodetection at the cavity output reduces the signal mode to a predetermined output state. The proposed setup can also be used to synthesize two-mode entangled states by using an additional Kerr medium, with possible applications in quantum information and quantum teleportation technology. The scheme works with high-Q cavities and conventional ON-OFF photodetectors, whereas it needs relatively large nonlinearities. These should be available in the next-future technology, since recent theoretical [4] and experimental [5] developments indicate that huge Kerr phase shifts of the order of 1 radiant per photon can be obtained through electromagnetic induced transparency.

2. Experimental apparatus and Fock state synthesis

The scheme, depicted in Fig. 1, is based on a ring cavity, coupled to the external radiation modes through two very low transmissivity τ beam splitters (BS) and a cross Kerr-medium. A tunable phase shifter, which shifts the field in the cavity by a phase ψ, is included in the device. One of the two cavity input modes (a_1) is pumped with a coherent source, while the other one (a_2) is left in the vacuum. Of the two output modes, one (b_2) is monitored with an ON-OFF photodetector D (which measures the presence or absence of the radiation field), the other one (b_1) is ignored, so that it is traced out. As will be shown in the following, whatever is the state of the input signal mode, a number state will be found at

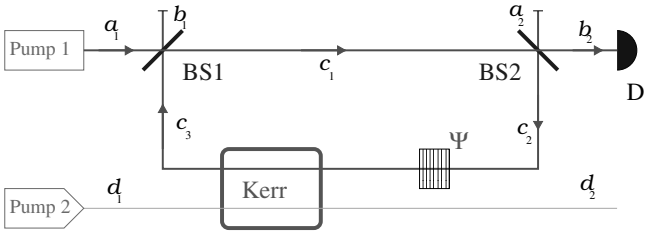

Fig. 1: Sketch of the experimental setup for the generation of optical Fock states in the traveling wave mode d_2, starting from two coherent pumps. The scheme is based on a conditional ON-OFF photodetector D, a non linear Cross–Kerr medium and a phase shifter ψ. The cavity input radiation modes are labelled a, the output modes b, the cavity modes c and the signal mode d. The quantum efficiency of the photodetector is not a crucial parameter, as it only affects the production rate of the device and not the quality of the generated states.

the output mode d_2 conditioned to a successful measurement at the detector D. Upon fulfillment of certain conditions shown in the following, superpositions of number states can also be generated. In principle, the specific number state (or superposition) that will be created is controlled by tuning the phase ψ.

We now show how the device works by analyzing the dynamics of its components in the Heisenberg picture. In principle, it would be necessary to quantize the field in the cavity starting from its classical equations of motion, as for example in [6]. However, we show that the same results are more easily obtained with a simple one mode model of the cavity, by simply identifying the output mode c_2 at the beam splitter BS2 with the input mode c_3 at BS1 (see Fig. 1). Let $a_{1,2}$ denote the two input modes for the ring cavity, $b_{1,2}$ the two output modes, c_1 the cavity mode exiting BS1, c_2 the cavity mode exiting BS2, c_3 the cavity mode exiting the Kerr medium and the phase shifter, and d_1 and d_2 the input and output signal mode respectively. In the Heisenberg picture, the input-output relations which characterize the components of the scheme are

$$\text{BS1:} \begin{cases} c_1 = \sqrt{\tau}\, a_1 + \sqrt{1-\tau}\, c_3 \\ b_1 = -\sqrt{1-\tau}\, a_1 + \sqrt{\tau}\, c_3 \end{cases}, \tag{2.1}$$

$$\text{BS2:} \begin{cases} c_2 = \sqrt{\tau}\, a_2 + \sqrt{1-\tau}\, c_1 \\ b_2 = -\sqrt{1-\tau}\, a_2 + \sqrt{\tau}\, c_1 \end{cases},$$

$$\text{Kerr and Phase shift: } c_3 = c_2 \exp\left[-i(\chi t\, d_1^\dagger d_1 - \psi)\right],$$

where τ is the transmissivity of the two beam splitters, χt is the Kerr susceptibility multiplicated by the interaction time, and ψ is the phase shift imposed to the cavity field mode by the phase shifter. From Eqs. (2.1) the output modes $b_{1,2}$ of the cavity can be expressed as a function of the input cavity and signal mode as

$$\begin{cases} b_1 = \kappa(\varphi)\, a_1 + e^{i\varphi}\, \sigma(\varphi)\, a_2 \\ b_2 = \sigma(\varphi)\, a_1 + \kappa(\varphi)\, a_2 \end{cases}, \quad \text{where} \quad \begin{cases} \kappa(\varphi) \doteq \dfrac{\sqrt{1-\tau}\,(e^{i\varphi}-1)}{1-(1-\tau)\,e^{i\varphi}} \\ \sigma(\varphi) \doteq \dfrac{\tau}{1-(1-\tau)\,e^{i\varphi}} \end{cases}, \tag{2.2}$$

where $\varphi \doteq -\chi t\, d_1^\dagger d_1 + \psi$ is the overall phase shift due to the Kerr medium and the phase shifter. Notice that the coupling with the signal mode is in the dependence of φ on the signal input mode d_1.

From the Heisenberg evolution of the modes (2.2), one obtains the state $|\Psi_{\rm out}\rangle$ in the cavity output modes (before the measurement) by using the creation operators $b_{1,2}^\dagger$ and by expressing the input state $|\Psi_{\rm in}\rangle$ on a Fock basis of the input modes $a_{1,2}$:

$$|\Psi_{\rm in}\rangle = \sum_{n,m=0}^{\infty} c_{nm}\, \frac{(a_1^\dagger)^n\,(a_2^\dagger)^m}{\sqrt{n!m!}}\, |0\rangle\,|0\rangle \rightarrow |\Psi_{\rm out}\rangle = \sum_{n,m=0}^{\infty} c_{nm}\, \frac{(b_1^\dagger)^n\,(b_2^\dagger)^m}{\sqrt{n!m!}}\, |0\rangle\,|0\rangle\ . \tag{2.3}$$

Consider the overall input state $\varrho_{\rm in}$ composed by a coherent state in mode a_1, vacuum in a_2 and generic state in d_1 (which will be described by the density matrix $\nu_{ss'}$ in the Fock basis), i.e.

$$\varrho_{\rm in} = |\alpha\rangle_{a_1a_1}\,\langle\alpha| \otimes |0\rangle_{a_2a_2}\,\langle 0| \otimes \sum_{s,s'=0}^{\infty} \nu_{ss'} |s\rangle_{d_1d_1}\,\langle s'|\,. \tag{2.4}$$

Through Eq. (2.3) we obtain the output state (before detection by detector D) on the modes $b_{1,2}$ and d_2 as

$$\begin{aligned}\varrho_{bd} &= |\alpha\kappa(\varphi)\rangle_{b_1b_1}\,\langle\alpha\kappa(\varphi)| \otimes |\alpha\, e^{i\varphi}\,\sigma(\varphi)\rangle_{b_2b_2}\,\langle\alpha\, e^{i\varphi}\sigma(\varphi)| \otimes \sum_{s,s'=0}^{\infty} \nu_{ss'} |s\rangle_{d_1d_1}\langle s'| \\ &= \sum_{s,s'=0}^{\infty} \nu_{ss'}\, |\alpha\kappa(\varphi_s)\rangle_{b_1b_1}\,\langle\alpha\kappa(\varphi_{s'})| \otimes |\alpha\, e^{i\varphi}\,\sigma(\varphi_s)\rangle_{b_2b_2}\,\langle\alpha\, e^{i\varphi}\,\sigma(\varphi_{s'})| \otimes |s\rangle_{d_2d_2}\,\langle s'|,\end{aligned} \tag{2.5}$$

where $\varphi_n \doteq -\chi t n + \psi$. After tracing out mode b_1, the state ϱ_{bd} becomes

$$\begin{aligned}\varrho'_{bd} = &\sum_{ss'} \nu_{ss'}\, e^{-\frac{|\alpha|^2}{2}[|\kappa(\varphi_s)|^2+|\kappa(\varphi_{s'})|^2-2\kappa(\varphi_s)\bar\kappa(\varphi_{s'})]} \\ &\times |\sigma(\varphi_s)\,\alpha\, e^{i\varphi}\rangle_{b_2b_2}\,\langle\sigma(\varphi_{s'})\,\alpha\, e^{i\varphi}\,| \otimes |s\rangle_{d_2d_2}\,\langle s'|\,,\end{aligned} \tag{2.6}$$

The state (2.6) now undergoes a reduction at detector D. An ON-OFF photodetector, with quantum efficiency η is described by the two value probability operator measure (POM)

$$\Pi_{\rm OFF} = \sum_{k=0}^{\infty} (1-\eta)^k\, |k\rangle\,\langle k|\,; \qquad \Pi_{\rm ON} = 1 - \Pi_{\rm OFF}\,, \tag{2.7}$$

which is obtained from the Mandel-Kelley-Kleiner formula [7]. The final state after the reduction in mode b_2, in the case of a successful (ON) photodetection is given by

$$\begin{aligned}\varrho_{\rm out} &= \frac{{\rm Tr}_{b_2}\,[\Pi_{\rm ON}\varrho_{bd}]}{{\rm Tr}\,[\Pi_{\rm ON}\varrho_{bd}]} \\ &= \frac{e^{-|\alpha|^2}}{\mathcal{N}} \sum_{s,s'=0}^{\infty} \nu_{ss'} \exp\,[|\alpha|^2\,(\kappa(\varphi_s)\,\kappa^*(\varphi_{s'}) + \sigma(\varphi_s)\,\sigma^*(\varphi_{s'})\,e^{i(\varphi_s-\varphi_{s'})})] \\ &\quad \times (1 - e^{-\eta|\alpha|^2\,\sigma(\varphi_s)\sigma^*(\varphi_{s'})})\,|s\rangle\,\langle s'|\,,\end{aligned} \tag{2.8}$$

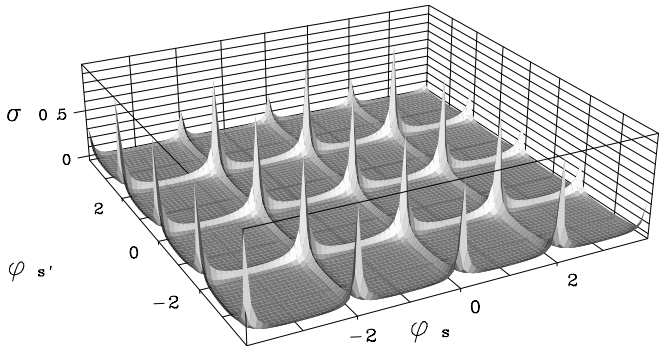

Fig. 2: Plot of the function $|\sigma(\varphi_s)\,\sigma^*(\varphi'_s)|$ [φ_s, $\varphi_{s'}$ in π units.], with $\tau = 0.1$, $n^* = \frac{\psi}{\chi t} = 0$ and $l^* = \frac{2\pi}{\chi t} = 2$. Notice the "fakir chair" structure: the function approaches a sum of delta functions for beam splitter transmissivity $\tau \to 0$.

where $\mathcal{N}$ is a normalization constant. Notice that the phase factors in the exponential in (2.8) do not play any role, as, in the working regime we exploit, these factors tend to one.

In the limit $\tau \to 0$, the effective transmissivity $\sigma(\varphi)$ of the cavity tends to a sum of Kronecker deltas

$$\lim_{\tau\to 0} |\sigma(\varphi_s)| = \begin{cases} 1 & \text{for} \quad \varphi_s \doteq -\chi t s + \psi = 2k\pi \ (k \in Z) \\ 0 & \text{for} \quad \varphi_s \neq 2k\pi \end{cases} = \sum_{k=-\infty}^{\infty} \delta_{s,\, kl^*+n^*} \,, \quad (2.9)$$

where $l^* = \frac{2\pi}{\chi t}$ is the distance between the peaks, and $n^* = \frac{\psi}{\chi t}$ is the position of the first peak. For the values of l^* and n^* for which the quantity $kl^* + n^*$ is not an integer, there is no contribution to the sum in (2.9). In Fig. 2 the function $|\sigma(\varphi_s)\,\sigma^*(\varphi'_s)|$ is plotted vs. φ_s and φ'_s.

From Eqs. (2.8) and (2.9) it is clear that for small values of the Kerr susceptibility χt (*i.e.* l^* high enough so that $\nu_{il^*+n^*,\, jl^*+n^*} \simeq 0$ for both i and j nonzero) and for high pump value $|\alpha| \gg 1$, the output state approaches a Fock state:

$$\lim_{\tau\to 0} \varrho_{\text{out}} = |n^*\rangle\,\langle n^*| \,. \quad (2.10)$$

Notice that the state $|n^*\rangle$ to be synthesized can be controlled by varying the phase ψ. In Fig. 3 the photon number distribution of the state (2.8), is given. Notice how the limiting case of Eq. (2.10) is approached.

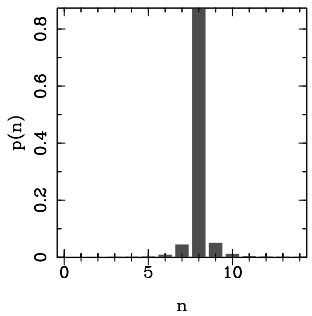

Fig. 3: Plot of photon number distribution of a synthesized Fock state. The experimental parameters are: $\tau = 0.01$, $\psi = 0.4$, $\chi t = 0.05$, $\eta = 10\%$ and the two pumps (in modes a_1 and d_1) are in a coherent state with amplitude $\alpha = \beta = 3$. The output state approaches a Fock state $|8\rangle$.

3. Other applications

Superposition generation. In order to produce superpositions of selected equally spaced number states, one has to provide higher values for the Kerr nonlinearity χt, or alternatively to provide sufficiently excited input state in mode d_1, so that the input state coefficients $\nu_{il^*+n^*,jl^*+n^*}$ are different from zero for different values of i and j. For example, as shown in Figs. 4 and 5, starting from a coherent input state with density matrix $\nu_{ss'} = e^{-|\beta|^2} \frac{\beta^s (\beta^*)^{s'}}{\sqrt{s!s'!}}$ it is possible to generate the superposition

$$|\Psi\rangle = \frac{1}{\sqrt{2}} \left(|n^*\rangle + e^{i\Phi} |n^* + l^*\rangle \right) \tag{3.11}$$

by choosing $|\beta|^2 = \sqrt[l^*]{\frac{(n^*-l^*)!}{n^*!}}$ and $\arg \beta = \frac{\Phi}{l^*}$. It must be stressed that only superpositions of the type

$$|\Psi\rangle = \sum_{k=0}^{\infty} c_k \, |n^* + kl^*\rangle \tag{3.12}$$

may be created, where the coefficients c_k are determined by the state incoming in mode d_1, i.e. by the coefficients $\nu_{ss'}$.

Photon number and state measurement. The proposed device can also be used for the measurement of the photon number distribution of an unknown quantum state. The probability of successful (ON) detection, in fact, is given by

$$P_{\mathsf{ON}} = \mathrm{Tr}\left[\Pi_{\mathsf{ON}} \rho_{bd}\right] = \sum_{k=0}^{\infty} \nu_{kk} (1 - e^{-\eta |\alpha|^2 |\sigma(\varphi_s)|^2}) \,, \tag{3.13}$$

and for sufficiently high l^* and $|\alpha| \gg 1$, is proportional to one of the diagonal elements of the input density matrix $P_{\mathsf{ON}} \simeq \nu_{n^* n^*}$. Thus, if an ensemble of identical states is impinged into the device in mode d_1, by tuning the cavity to different values of n^* and measuring the relative frequency of ON photodetection, one can obtain $\nu_{n^* n^*}$. This allows the measurement of the photon number distribution of an arbitrary state, using less experimental data

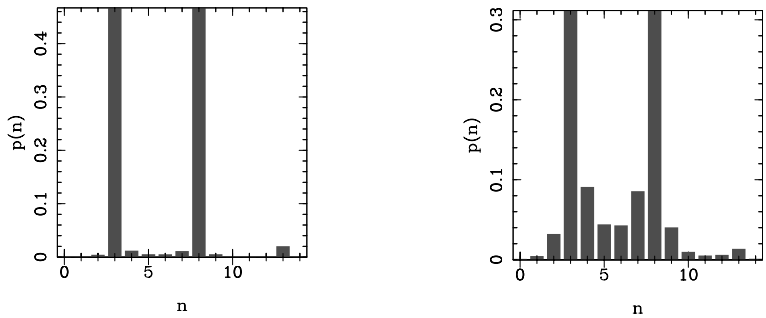

Fig. 4: Plot of the diagonal of the density matrix ϱ_{out} exiting the device for a coherent input in mode d_1 with modulus $|\beta|^2 = \sqrt[5]{\frac{8!}{3!}}$ and with $l^* = 5$, $n^* = 3$. The parameters are chosen so to have the superposition $\frac{1}{\sqrt{2}}(|3\rangle + |8\rangle)$. In the left plot, notice a residual component at the Fock state 13, which results from the term $k = 2$ in the sum (2.9). Here, the quantum efficiency of detector D is $\eta = 10\%$, the modulus of the cavity pump is $\alpha = 8$, the BS transmissivity is $\tau = 0.06$. In the right plot we used $\tau = 0.2$, to show the smearing effect of a bad cavity.

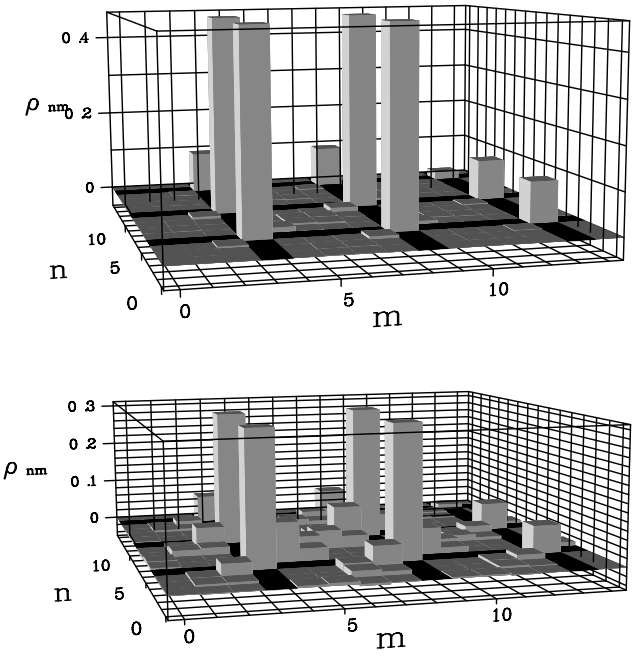

Fig. 5: Density matrix for the two states given in Fig. 4

and lower quantum efficiency detectors than in homodyne tomography (which is the currently used experimental procedure for reconstructing the number distribution of arbitrary states). Moreover, by using the least-squares inversion method outlined in [9] and by displacing the input state with a beam splitter, it is possible to reconstruct also the truncated density matrix of the state in the Fock basis. The details for such an experimental setup will be given elsewhere.

Entanglement creation. A modified version of the proposed experiment may also be used for the production of two-mode entangled states. One only has to use two Kerr crystals inside the cavity, as shown in Fig. 6. In this case, the total phase shift imposed by the cavity is given by the sum of the effect of each Kerr medium. For identical Kerr crystals $K1$ and $K2$ (i.e. $\chi_{K1} \equiv \chi_{K2} \doteq \chi$), one has $l^* = \frac{\pi}{\chi t}$ and $n^* = \frac{\psi}{2\chi t} = n_1^* + n_2^*$, where n_1^* and n_2^* are the eigenvalues of the number states in the modes $d^{(1)}$ and $d^{(2)}$ impinging into each of

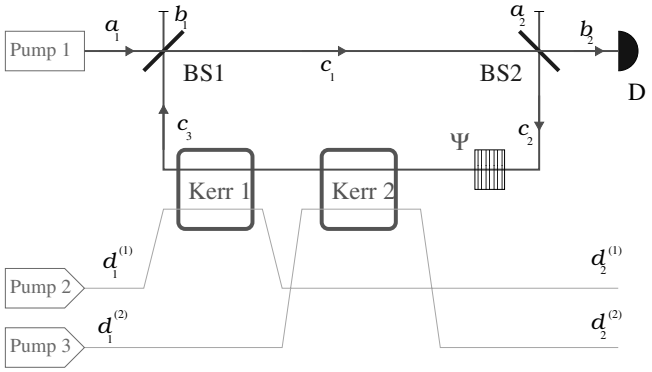

Fig. 6: Modification of the proposed experimental setup, in order to construct entangled states between the output modes $d_2^{(1)}$ and $d_2^{(2)}$.

the Kerr crystals. In this case, Eq. (2.9) becomes

$$\lim_{\tau\to 0} |\sigma(\varphi_s)| = \sum_k \delta_{s,\, kl^*+n_1^*+n_2^*} \,, \tag{3.14}$$

and the output state (2.10) for $\tau \ll 1$ and $|\alpha| \gg 1$ now reads

$$\varrho_{\text{out}} = \sum_{n,\,k=0}^{n^*} \nu_{nk}^{(1)} \nu_{nk}^{(2)} \, |n\rangle_{d_2^{(1)} d_2^{(1)}} \langle k| \otimes |n^*-n\rangle_{d_2^{(2)} d_2^{(2)}} \langle n^*-k| \,, \tag{3.15}$$

that is obtained in the limit of low Kerr nonlinearity $\chi t \ll 1$ (i.e. $l^* \gg 1$). For input signal pure states $|\Psi_{\text{in}}\rangle = \sum_k \nu_k^{(1)} |k\rangle_{d_1^{(1)}} \otimes \sum_j \nu_j^{(2)} |j\rangle_{d_1^{(2)}}$, one finds

$$|\Psi_{\text{out}}\rangle = \sum_{k=0}^{n^*} \nu_k^{(1)} \nu_{n^*-k}^{(2)} \, |k\rangle_{d_2^{(1)}} \, |n^*-k\rangle_{d_2^{(2)}} \,. \tag{3.16}$$

It is obvious that any multipartite entanglement between many modes could be synthesized in principle, by increasing the number of Kerr media in the cavity. This method could then be used also to generate Greenberger–Horn–Zeilinger states.

4. Feasibility

We now analyze the effect of detector's D quantum efficiency. As can be seen from Fig. 7, lowering the detector's quantum efficiency actually purifies the state. Qualitatively this can be explained by noticing that in Eq. (2.8) the lowering of η contributes to the convergence exploited in Eq. (2.10) to produce the Fock state (or the superpositions). It would seem that one could actually increase the output signal quality by using low efficiency photodetectors. The drawback is given in terms of production rate of the desired Fock states. It is obvious that it is less probable for a non-efficient photodetector to click, so the production rate is drastically decreased. In fact, the probability of a successful ON photodetection is given by Eq. (3.13), from which one can see that P_{ON} exponentially decreases with decreasing η,

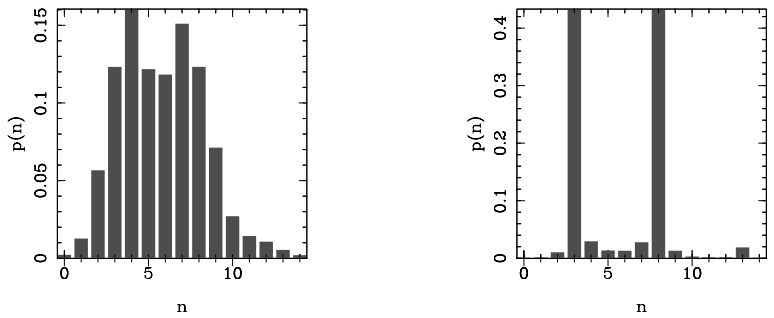

Fig. 7: Plots for the same parameters as for the right Figure 4 (i.e. $|\beta|^2 = \sqrt[5]{\frac{8!}{3!}}$, $l^* = 5$, $n^* = 3$, $\alpha = 8$ and $\tau = 0.2$). On the left $\eta = 100\%$, while on the right $\eta = 1\%$. This show-show lowering the detector's quantum efficiency enhances the quality of the state. The cost is paid in terms of a lower production rate: the probability (3.13) of obtaining the state depicted on the left is $P_{\text{ON}} \simeq 0.789$, while on the right $P_{\text{ON}} \simeq 0.106$.

and which for $\tau \to 0$ and $|\alpha| \gg 1$ tends to

$$P_{\mathsf{ON}} \to \sum_{k=0}^{\infty} \nu_{kl^*+n^*,\, kl^*+n^*} \,. \tag{4.17}$$

The quantum efficiency η of the detector in the proposed device is, therefore, not a critical parameter, so that ordinary photodetectors may be used in the experimental setup. Using low efficiency photodetection does not reduce the quality of the output states, but only it affects their production rate.

The actual feasibility of the proposed experimental setup relies on the availability of good ring cavities, suitable Kerr nonlinearities, and ordinary photodetection. The cavity couples to the outside modes through small transmissivity beam splitters $\tau \simeq 0.1 \div 0.01\%$. The Kerr nonlinearities that are needed are of the order of $\chi t \simeq 0.01$ for the creation of number states and of the order of $\chi t \simeq 0.1$ for obtaining superpositions. Photodetection with quantum efficiency as low as $\eta = 1\%$ has been shown to be effective. The output state must be controlled by varying the phase shift ψ which can be varied, in ordinary experimental setups, in steps of the order of $\frac{\pi}{500}$ [8]. To our knowledge, the experiment for the generation of Fock states or two mode entangled states should be feasible with laboratory technology now available. The creation of Fock state superposition may ask for Kerr nonlinearities which are not yet available in the optical domain, though recent results [4, 5] indicate that giant non-linear shifts of the order of 1 radiant per photon may be obtained through electromagnetically induced transparency.

5 Conclusions

In conclusion we have proposed an optical device capable of creating optical Fock states, selected superposition of Fock states, and two mode entangled states. The experimental setup is composed of a high-Q ring cavity coupled with the signal mode through a cross-Kerr medium and an ON-OFF photodetection. A successful photodetection reduces the signal mode to a predetermined output state. We have shown that imperfect photodetection does not affect the quality of the output states. The same device can be also used for the measurement of the photon number distribution and of the density matrix in the Fock basis. The applications for such a device in the modern "Quantum technology" are numerous and span through many of the fields of advanced quantum optics research.

References

[1] H. P. YUEN and M. OZAWA, Phys. Rev. Lett. **70**, 363 (1993).
[2] I. L. CHUANG and Y. YAMAMOTO, Phys. Rev. A **52**, 3489 (1995).
[3] G. M. D'ARIANO, L. MACCONE, Phys. Rev. Lett. **80**, 5465 (1998).
[4] H. SCHMIDT and A. IMAMOGLU, Opt. Lett. **21**, 1936 (1996); H. SCHMIDT and A. IMAMOGLU, Opt. Lett. **23**, 1007 (1998).
[5] L. V. HAU, S. E. HARRIS, Z. DUTTON and C. H. BEHROOZI, Nature **397**, 594 (1999).
[6] M. LEY and R. LOUDON, J. Mod. Opt. **34**, 227 (1987).
[7] P. L. KELLEY and W. H. KLEINER, Phys. Rev. A **30**, 844 (1964).
[8] O. HADERKA, M. HENDRYCH, private communication.
[9] T. OPATRNÝ and D.-G. WELSCH, Phys. Rev. A **55**, 1462 (1997).